Contribution from AT&T Bell Laboratories,
Murray Hill, New Jersey 07974

# Atomic Arrangements and Electronic Requirements for Close-Packed Circular and Spherical Clusters

Boon K. Teo*† and N. J. A. Sloane*

*Received May 21, 1985*

This paper gives results concerning the numbers and types of atoms and their coordinates in closed-shell, close-packed clusters as a function of the nuclearity (or magic numbers). The clusters studied are circular clusters in the square and hexagonal lattices in two dimensions and spherical clusters in the simple, face-centered and body-centered cubic lattices and the hexagonal close packing in three dimensions, for various choices for the center of the cluster. These *atom-counting* results are applied to *electron counting* of high-nuclearity close-packed metal cluster systems, cluster beams, catalysis, surface science, EXAFS, LEED, and other structural techniques.

## Introduction

High-nuclearity clusters often adopt a symmetrical and more or less spherical shape. In a previous paper[1] we developed a general method based on *theta series* for calculating the numbers and types of atoms in circular and spherical closed-shell, close-packed clusters, gave general expressions for their coordinates, and determined their symmetry groups. The present paper studies *particular* examples of these clusters in more detail and gives explicit coordinates for the atoms and some figures illustrating the disposition of the atoms in the first few shells. We shall refer to these results as *atom counting*. For example, what would a symmetrical *closed-shell* and *close-packed spherical* cluster of 201 atoms look like? What would be its electronic requirements? Such questions are important in the design and understanding of cluster systems. We shall also discuss the applications of the atom-counting results to metal cluster chemistry, *electron counting* of metal cluster systems, cluster beams, catalysis, surface science and related spectroscopic or structural techniques, and other topics. It is hoped that the present work will not only serve as a guide to close-packed cluster architecture but will also stimulate further research in cluster chemistry and related disciplines.

## Lattices and Magic Numbers

The lattices considered are the square and hexagonal lattices in 2D and the simple cubic, face-centered cubic (FCC), and body-centered cubic (BCC) lattices and the hexagonal close-packing (HCP) arrangement in 3D. We place the origin of coordinates at some point of the space (but not necessarily at the center of an atom). The atoms can now be classified according to their distance from the origin, and we let $S_n$ denote the number of atoms at distance $n^{1/2}$ from the origin. These $S_n$ atoms form a "shell" of radius $n^{1/2}$. Then the set of all atoms inside or on this shell forms a *close-packed circular* (2-D) or *spherical* (3-D) *cluster*, centered at the origin, containing a total of

$$G_n = \sum_{m \le n} S_m \qquad (1)$$

atoms (the *nuclearity* or *magic number*). The most interesting clusters are those that possess nontrivial symmetries, and we shall therefore only consider clusters centered at points such as a lattice point (i.e. the center of an atom), a point midway between two adjacent atoms (if adjacent atoms are joined by edges, this is the midpoint of an edge), a point equidistant from three or four mutually adjacent atoms, if such a point exists (i.e. the center of a triangle or square), and a *hole*[2] (i.e. a point maximally distant from the adjacent atoms).

The clusters are described in Tables I–XXVII. The tables give, for each lattice and each choice for the center of the cluster, the following information. The first column gives the squared distance ($n$) of the shell from the origin, and the second column gives the coordinates of the atoms in that shell. Note that only one representative is given for each equivalent class of coordinates under the action of the symmetry group of the cluster. The full set of atomic coordinates is obtained from the representatives given by applying the permutations and sign changes specified in the previous paper.[1] For example, the 21 entry for $n = 5$ in Table

Table I.

| $n$ | coords. | $S_n$ | $G_n$ |
|---|---|---|---|
| 0 | 00 | 1 | 1 |
| 1 | 10 | 4 | 5 |
| 2 | 11 | 4 | 9 |
| 4 | 20 | 4 | 13 |
| 5 | 21 | 8 | 21 |
| 8 | 22 | 4 | 25 |
| 9 | 30 | 4 | 29 |
| 10 | 31 | 8 | 37 |
| 13 | 32 | 8 | 45 |
| 16 | 40 | 4 | 49 |
| 17 | 41 | 8 | 57 |
| 18 | 33 | 4 | 61 |

Table II.

| $n$ | coords.* |
|---|---|
| 1/4 | 10 |
| 1 1/4 | 12 |
| 2 1/4 | 30 |
| 3 1/4 | 32 |
| 4 1/4 | 14 |
| 6 1/4 | 50[2], 34[4] |
| 7 1/4 | 52 |
| 9 1/4 | 16 |
| 10 1/4 | 54 |
| 11 1/4 | 36 |
| 12 1/4 | 70 |
| 13 1/4 | 72 |

Table III.

| $n$ | coords.* |
|---|---|
| 1/2 | 11 |
| 2 1/2 | 31 |
| 4 1/2 | 33 |
| 6 1/2 | 51 |
| 8 1/2 | 53 |
| 12 1/2 | 71[8], 55[4] |
| 14 1/2 | 73 |
| 18 1/2 | 75 |
| 20 1/2 | 91 |
| 22 1/2 | 93 |
| 24 1/2 | 77 |
| 26 1/2 | 95 |

Table I. Square lattice $\mathbf{Z}^2$ with respect to lattice point.

Table II. $\mathbf{Z}^2$ with respect to mid-point of edge. [When there is more than one type of point with the same norm, the number of points of each type is given in square brackets.] *Coords. have been multiplied by 2.

Table III. $\mathbf{Z}^2$ with respect to center of square. *Coords. have been multiplied by 2.

Table IV.

| $n$ | coords. | $S_n$ | $G_n$ |
|---|---|---|---|
| 0 | 000 | 1 | 1 |
| 2 | $\bar{1}10$ | 6 | 7 |
| 6 | $\bar{2}11$ | 6 | 13 |
| 8 | $\bar{2}20$ | 6 | 19 |
| 14 | $\bar{3}21$ | 12 | 31 |
| 18 | $\bar{3}30$ | 6 | 37 |
| 24 | $\bar{4}22$ | 6 | 43 |
| 26 | $\bar{4}31$ | 12 | 55 |
| 32 | $\bar{4}40$ | 6 | 61 |
| 38 | $\bar{5}32$ | 12 | 73 |
| 42 | $\bar{5}41$ | 12 | 85 |
| 50 | $\bar{5}50$ | 6 | 91 |

Table V.

| $n$ | coords.* |
|---|---|
| 1/2 | $\bar{1}10$ |
| 1 1/2 | $\bar{1}12$ |
| 3 1/2 | $\bar{3}12$ |
| 4 1/2 | $\bar{3}30$ |
| 6 1/2 | $\bar{3}14$ |
| 9 1/2 | $\bar{5}32$ |
| 10 1/2 | $\bar{5}14$ |
| 12 1/2 | $\bar{5}50$ |
| 13 1/2 | $\bar{3}36$ |
| 15 1/2 | $\bar{5}16$ |
| 18 1/2 | $\bar{7}34$ |
| 19 1/2 | $\bar{7}52$ |

Table VI.

| $n$ | coords.* |
|---|---|
| 2/3 | $\bar{2}11$ |
| 2 2/3 | $\bar{4}22$ |
| 4 2/3 | $\bar{5}41$ |
| 8 2/3 | $\bar{7}52$ |
| 10 2/3 | $\bar{8}44$ |
| 12 2/3 | $\bar{8}71$ |
| 16 2/3 | $\bar{10}55$ |
| 18 2/3 | $\bar{10}82$ |
| 20 2/3 | $\bar{11}74$ |
| 24 2/3 | $\bar{11}10\,1$ |
| 28 2/3 | $\bar{13}85$ |

Table IV. $A_2$ with respect to lattice point.

Table V. $A_2$ with respect to mid-point of edge. *Coords. have been multiplied by 2.

Table VI. $A_2$ with respect to center of triangle. *Coords. have been multiplied by 3.

†Present address: Department of Chemistry, University of Illinois, Chicago, IL 60680.

(1) Sloane, N. J. A.; Teo, B. K. *J. Chem. Phys.* **1985**, *83*, 6520.
(2) (a) Conway, J. H.; Parker, R. A.; Sloane, N. J. A. *Proc. R. Soc. London, Ser. A* **1982**, *380*, 261. (b) Conway, J. H.; Sloane, N. J. A. *Ann. Math.* **1982**, *116*, 593. A *deep* hole is a point maximally distant from the lattice, while a *shallow* hole is only locally maximally distant from the lattice. For example the FCC has both deep (or octahedral) and shallow (or tetrahedral) holes.

0020-1669/86/1325-2315$01.50/0 

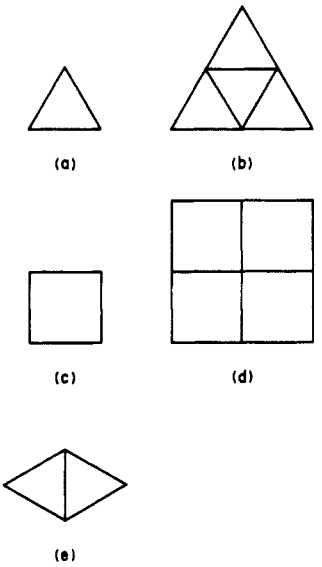


**Figure 1.** (a) $\nu_1$ triangle. (b) $\nu_2$ triangle. (c) $\nu_1$ square. (d) $\nu_2$ square. (e) Two triangles with a common edge.

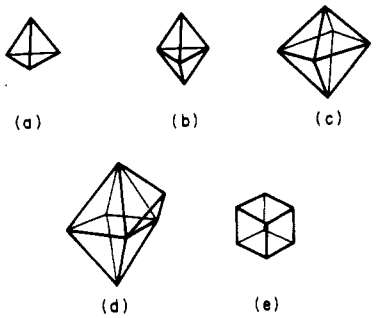


**Figure 2.** (a) Tetrahedron. (b) Triangular bipyramid. (c) Octahedron. (d) Monocapped octahedron. (e) Cube.

I represents eight atoms at (±2, ±1) and (±1, ±2). When there is more than one type of atom with the same norm, the numbers of atoms of each type are given in brackets. For clusters centered at a lattice point, the third column gives $S_n$, the number of atoms in the shell, and the last column gives the magic number $G_n$ (see eq 1). More extensive tables of $S_n$ and $G_n$ for all these clusters will be found in ref 1.

The tables were calculated by using the methods described in the previous paper.[1]

## Results and Discussion

We shall now discuss some of the known clusters to be found in the tables. Despite tremendous efforts by many groups over the last decades only the early members of these series are presently known in metal cluster chemistry. We hope that the tables presented in this paper will be useful guides to higher circular (2D) and spherical (3D) cluster geometries and that those in ref 3 will be useful for understanding the architecture and atomic arrangement of polygonal and polyhedral clusters.

**Examples in Metal Cluster Chemistry.** Table XXVIII lists some of the clusters that are known in metal cluster chemistry. The list is meant to be illustrative rather than exhaustive. Furthermore, we include only values of $G_n \geq 3$ for 2D and $G_n \geq 4$ for 3D clusters. Cluster that occur in several series will be mentioned only once.

The $\nu_1$ (Figure 1a) and $\nu_2$ (Figure 1b) triangles are known in, e.g., $Os_3(CO)_{12}$[4] and $Os_6(CO)_{17}(P(OMe)_3)_4$,[5] respectively. These are the earliest clusters in the hexagonal ($A_2$) lattice centered at the center of a triangle (cf. Table VI). For the same lattices

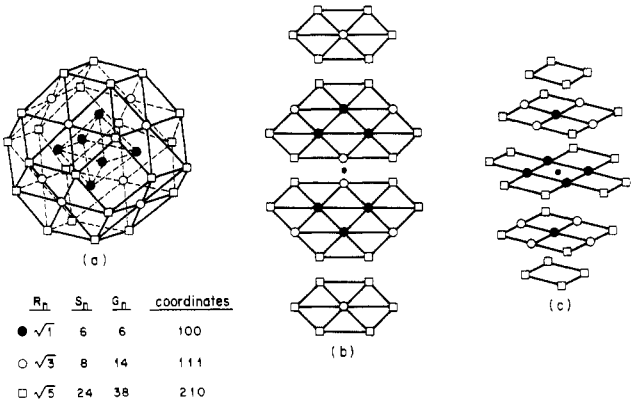


**Figure 3.** Three views of a 38-point cluster in FCC lattice centered at an octahedral hole, forming a $\nu_1$ truncated octahedron.

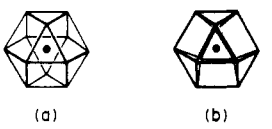


**Figure 4.** (a) Cuboctahedron. (b) Twinned cuboctahedron.

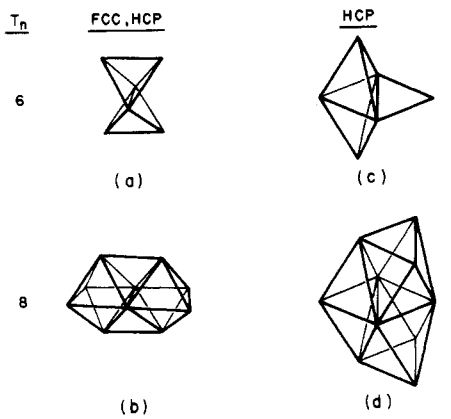


**Figure 5.** (a) Edge-sharing bitetrahedron. (b) Edge-sharing bioctahedron. (c) Edge-capped triangular bipyramid. (d) Fused face-sharing bioctahedron and triangular bipyramid.

centered at the midpoint of an edge (cf. Table V), we have the planar parallelogram shown in Figure 1e, which is found in $[Re_4(CO)_{16}]^{2-}$.[6] This structure is best described as two triangles sharing a common edge. The $\nu_1$ (Figure 1c) square is found in, e.g., $CO_4(PPh)_2(CO)_{10}$.[7] The $\nu_2$ (Figure 1d) square is not yet known in metal cluster chemistry. However, the related $\nu_2$ parallelogram has recently been observed in the $Cu_5Fe_4(CO)_{16}^{3-}$ trianion.[8] Note that the $\nu_2$ parallelogram does not belong to any of the series considered here (since it is *not* a circular polygon).

The simple cubic structure found in $Ni_8(PPh)_6(CO)_8$[9] (Figure 2e) is the first member of the series derived from the simple cubic lattice centered at a cubic hole (Table X).

The simple tetrahedral structure (Figure 2a), which is exemplified by $Ir_4(CO)_{12}$,[10] can be found in many series (cf. Tables XIII, XIV, and XXII). It is interesting to note that the highly symmetrical $\nu_2$ tetrahedral structure, found in $[Os_{10}C(CO)_{24}]^{2-}$[11] and discussed in ref 3, does not belong to any of the series considered here. It is *not* a spherical cluster.

(3) Teo, B. K.; Sloane, N. J. A. *Inorg. Chem.* **1985**, *24*, 4545.
(4) (a) Corey, E. R.; Dahl, L. F. *Inorg. Chem.* **1962**, *1*, 521. (b) Churchill, M. R.; DeBoer, B. G. *Inorg. Chem.* **1977**, *16*, 878.
(5) Goudsmit, R. J.; Johnson, B. F. G.; Lewis, J.; Raithby, P. R. Whitmire, K. *J. Chem. Soc., Chem. Commun.* **1982**, 640.
(6) Churchill, M. R.; Bau, R. *Inorg. Chem.* **1968**, *7*, 2606.
(7) Ryan, R. C.; Dahl, L. F. *J. Am. Chem. Soc.* **1975**, *97*, 6904.
(8) Doyle, G.; Eriksen, K. A.; Van Engen, D. *J. Am. Chem. Soc.* **1985**, *107*, 7914.
(9) Lower, L. D.; Dahl, L. F. *J. Am. Chem. Soc.* **1976**, *98*, 5046.
(10) Churchill, M. R.; Hutchinson, J. P. *Inorg. Chem.* **1978**, *17*, 3528 and references cited therein.
(11) Jackson, P. F.; Johnson, B. F. G.; Lewis, J.; Nelson, W. J. H.; McPartlin, M. *J. Chem. Soc., Dalton Trans.* **1982**, 2099.

**Table VII.**

| $n$ | coords. | $S_n$ | $G_n$ |
|---|---|---|---|
| 0 | 000 | 1 | 1 |
| 1 | 100 | 6 | 7 |
| 2 | 110 | 12 | 19 |
| 3 | 111 | 8 | 27 |
| 4 | 200 | 6 | 33 |
| 5 | 210 | 24 | 57 |
| 6 | 211 | 24 | 81 |
| 8 | 220 | 12 | 93 |
| 9 | 300[6], 221[24] | 30 | 123 |
| 10 | 310 | 24 | 147 |
| 11 | 311 | 24 | 171 |
| 12 | 222 | 8 | 179 |

Table VII. $\mathbf{Z}^3$ with respect to lattice point.

**Table VIII.**

| $n$ | coords.* |
|---|---|
| 1/4 | 100 |
| 1 1/4 | 120 |
| 2 1/4 | 300[2], 122[8] |
| 3 1/4 | 320 |
| 4 1/4 | 322[8], 140[8] |
| 5 1/4 | 142 |
| 6 1/4 | 500[2], 340[8] |
| 7 1/4 | 520[8], 342[16] |
| 8 1/4 | 522[8], 144[8] |
| 9 1/4 | 160 |
| 10 1/4 | 540[8], 344[8], 162[16] |
| 11 1/4 | 542[16], 360[8] |

Table VIII. $\mathbf{Z}^3$ with respect to mid-point of edge. *Coords. have been multiplied by 2.

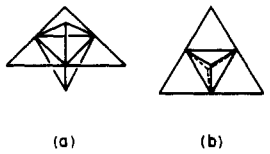


**Figure 6.** Two views of a edge-capped triangular bipyramid.

The third member of the FCC series centered at the center of a triangle (Table XIII) is the monocapped octahedron (Figure 2d) found in, e.g., $[Rh_7(CO)_{16}]^{3-}$.[12]

The first three members of the series derived from the FCC lattice centered at an octahedral hole (Table XV) are the octahedron (Figure 2c), the octacapped octahedron, and the truncated $\nu_3$ octahedron (cf. Figure 3) as examplified by $Rh_6(CO)_{16}$,[13] $\underline{Ti}_6O_8Cp_6$,[14] and $[Pt_{38}(CO)_{44}H_x]^{2-}$,[15] respectively.

The first nontrivial member of the series derived from the FCC centered at a lattice point is the 13-atom cuboctahedron shown in Figure 4a. This structure is at present not known in metal cluster chemistry. The equivalent in the HCP, the twinned cuboctahedron (Figure 4b), has been observed in $[Rh_{13}(CO)_{24}H_{5-n}]^{n-}$.[16]

We shall now discuss the FCC and HCP centered at the midpoint of an edge. The first two nontrivial members of both series are depicted in Figure 5. In the FCC, all edges are equivalent, and we have only one series as shown in Table XII. The hexanuclear edge-sharing bitetrahedron (Figure 5a) and the decanuclear edge-sharing bioctahedron (Figure 5b) are exemplified by $(Ph_3P)_2Au_2Os_4H_2(CO)_{12}$[17] and $[Ru_{10}C_2(CO)_{24}]^{2-}$,[18] respectively. There are, on the other hand, two kinds of edges in the HCP: those within the hexagonal layers (Table XVII) and those between layers (Table XVIII). The early members (and only the early members) of the latter series are the same as those of the FCC series (Table XII), which have already been illustrated in Figure 5a,b. The former series (Table XVII) gives rise to an edge-capped triangular bipyramid (Figure 5c) and a fused face-sharing bioctahedron and triangular bipyramid (Figure 5d).

It is important to note that, in the FCC, the tetrahedral and the octahedral holes alternate so that there is only one type of lattice point, edge, triangle, square, tetrahedral hole, and octahedral hole. In the HCP, on the other hand, each tetrahedral hole is surrounded by *one* tetrahedral hole and *three* octahedral holes, while each octahedral hole is surrounded by *two* octahedral holes and *six* tetrahedral holes. As a result there are, in addition to the two kinds of edges discussed earlier, three types of triangles: those adjacent to two tetrahedral holes, those adjacent to two octahedral holes, and those between layers. We call these three types of triangles "tetrahedral" (Table XIX), "octahedral" (Table XX), and "triangles between layers" (Table XXI). Table XIX lists the series derived from the HCP centered at the midpoint of a "tetrahedral" triangle (see ref 1 for the magic numbers). The pentanuclear trigonal-bipyramidal structure (Figure 2b) is exemplified by $Os_5(CO)_{16}$.[19] The next member, the octanuclear

**Table IX.**

| $n$ | coords.* |
|---|---|
| 1/2 | 110 |
| 1 1/2 | 112 |
| 2 1/2 | 310 |
| 3 1/2 | 312 |
| 4 1/2 | 330[4], 114[8] |
| 5 1/2 | 332 |
| 6 1/2 | 510[8], 314[16] |
| 7 1/2 | 512 |
| 8 1/2 | 530[8], 334[8] |
| 9 1/2 | 532[16], 116[8] |
| 10 1/2 | 514 |
| 11 1/2 | 316 |

Table IX. $\mathbf{Z}^3$ with respect to center of square face. *Coords. have been multiplied by 2.

**Table X.**

| $n$ | coords.* |
|---|---|
| 3/4 | 111 |
| 2 3/4 | 311 |
| 4 3/4 | 331 |
| 6 3/4 | 511[24], 333[8] |
| 8 3/4 | 531 |
| 10 3/4 | 533 |
| 12 3/4 | 711[24], 551[24] |
| 14 3/4 | 731[48], 553[24] |
| 16 3/4 | 733 |
| 18 3/4 | 751[48], 555[8] |
| 20 3/4 | 911[24], 753[48] |
| 22 3/4 | 931 |

Table X. $\mathbf{Z}^3$ with respect to center of cube. *Coords. have been multiplied by 2.

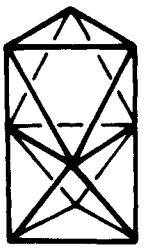

**Figure 7.** Face-sharing bioctahedron.

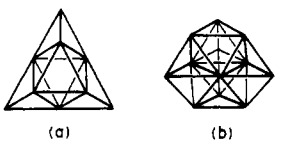


**Figure 8.** Two views of a bidiminished $\nu_2$ triangular bipyramid.

**Figure 9.** Hexacapped octahedron.

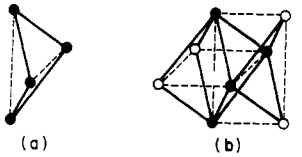


**Figure 10.** First two clusters in the BCC lattice centered at a tetrahedral hole.


(12) Albano, V. G.; Bellon, P. L.; Ciani, G. F. *J. Chem. Soc., Chem. Commun.* **1969**, 1024.
(13) Corey, E. R.; Dahl, L. F.; Beck, W. *J. Am. Chem. Soc.* **1963**, *85*, 1202.
(14) Huffman, J. C.; Stone, J. G.; Krusell, W. C.; Caulton, K. G. *J. Am. Chem. Soc.* **1977**, *99*, 5829.
(15) Ceriotti, A.; Washecheck, D.; Dahl, L. F.; Longoni, G.; Chini, P., private communication.
(16) Ciani, G.; Sironi, A.; Martinengo, S. *J. Chem. Soc., Dalton Trans.* **1981**, 519.
(17) Johnson, B. F. G.; Kaner, D. A.; Lewis, J.; Raithby, P. R.; Taylor, M. J. *Polyhedron* **1982**, *1*, 105.
(18) Hayward, C. T.; Shapley, J. R.; Churchill, M. R.; Bueno, C.; Rheingold, A. L. *J. Am. Chem. Soc.* **1982**, *104*, 7347.
(19) Eady, C. R.; Johnson, B. F. G.; Lewis, J.; Reichert, B. E.; Sheldrick, G. M. *J. Chem. Soc., Chem. Commun.* **1976**, 271.

Table XI.

| $n$ | coords. | $S_n$ | $G_n$ |
|---|---|---|---|
| 0 | 000 | 1 | 1 |
| 2 | 110 | 12 | 13 |
| 4 | 200 | 6 | 19 |
| 6 | 211 | 24 | 43 |
| 8 | 220 | 12 | 55 |
| 10 | 310 | 24 | 79 |
| 12 | 222 | 8 | 87 |
| 14 | 321 | 48 | 135 |
| 16 | 400 | 6 | 141 |
| 18 | 330[12], 411[24] | 36 | 177 |
| 20 | 420 | 24 | 201 |
| 22 | 422 | 24 | 225 |

Table XII.

| $n$ | coords.* |
|---|---|
| $\frac{1}{2}$ | 110 |
| $1\frac{1}{2}$ | $1\bar{1}2$ |
| $2\frac{1}{2}$ | $3\bar{1}0$ |
| $3\frac{1}{2}$ | 312 |
| $4\frac{1}{2}$ | 330[2], 114[4] |
| $5\frac{1}{2}$ | $3\bar{3}2$ |
| $6\frac{1}{2}$ | 510[4], $3\bar{1}4$[8] |
| $7\frac{1}{2}$ | $5\bar{1}2$ |
| $8\frac{1}{2}$ | $5\bar{3}0$[4], 334[4] |
| $9\frac{1}{2}$ | 532[8], $1\bar{1}6$[4] |
| $10\frac{1}{2}$ | 514 |
| $11\frac{1}{2}$ | 316 |

Table XIII.

| $n$ | coords.* |
|---|---|
| $\frac{2}{3}$ | $\bar{2}11$ |
| $1\frac{1}{3}$ | $\bar{2}\bar{2}\bar{2}$ |
| 2 | $4\bar{1}1$ |
| $2\frac{2}{3}$ | $4\bar{2}\bar{2}$ |
| $3\frac{1}{3}$ | $5\bar{2}1$ |
| 4 | $44\bar{2}$ |
| $4\frac{2}{3}$ | $\bar{5}41$ |
| $5\frac{1}{3}$ | 444 |
| 6 | $7\bar{2}1$[6], $\bar{5}\bar{5}2$[3] |
| $7\frac{1}{3}$ | $\bar{8}11$[3], 741[6] |
| | $\bar{5}\bar{5}4$[3] |
| 8 | $\bar{8}\bar{2}\bar{2}$ |

Table XIV.

| $n$ | coords.* |
|---|---|
| $\frac{3}{4}$ | $\bar{1}11$ |
| $2\frac{3}{4}$ | $\bar{3}11$ |
| $4\frac{3}{4}$ | $\bar{3}31$ |
| $6\frac{3}{4}$ | $\bar{5}11$[12], 333[4] |
| $8\frac{3}{4}$ | $\bar{5}31$ |
| $10\frac{3}{4}$ | $\bar{5}33$ |
| $12\frac{3}{4}$ | $\bar{7}11$[12], $\bar{5}51$[12] |
| $14\frac{3}{4}$ | $\bar{7}31$[24], 553[12] |
| $16\frac{3}{4}$ | $733\bar{}$ |
| $18\frac{3}{4}$ | $\bar{7}51$[24], $\bar{5}55$[4] |
| $20\frac{3}{4}$ | $\bar{9}11$[12], 753[24] |
| $22\frac{3}{4}$ | 931 |

Table XV.

| $n$ | coords. |
|---|---|
| 1 | 100 |
| 3 | 111 |
| 5 | 210 |
| 9 | 300[6], 221[24] |
| 11 | 311 |
| 13 | 320 |
| 17 | 410[24], 322[24] |
| 19 | 331 |
| 21 | 421 |
| 25 | 500[6], 430[24] |
| 27 | 333[8], 511[24] |
| 29 | 520[24], 432[48] |

Table XI. FCC with respect to lattice point.

Table XII. FCC with respect to mid-point of edge. *Coords. have been multiplied by 2.

Table XIII. FCC with respect to center of triangle. *Coords. have been multiplied by 3.

Table XIV. FCC with respect to center of tetrahedral hole. *Coords. have been multiplied by 2.

Table XV. FCC with respect to center of octahedral hole.

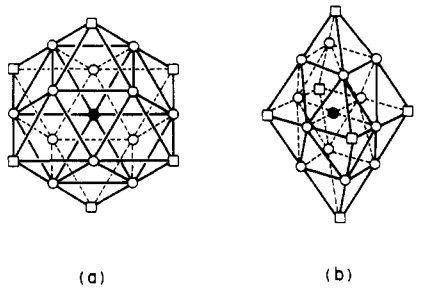


**Figure 11.** Two views of a 19-point spherical cluster in the FCC lattice forming a $\nu_2$ octahedron.

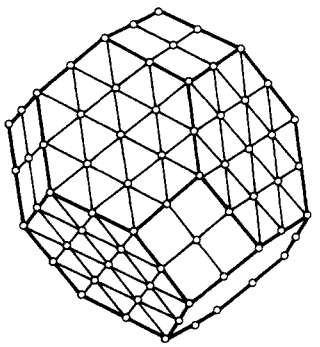

**Figure 12.** The 201-point spherical cluster in the FCC lattice forming a $\nu_2$ truncated octahedron.

edge-capped triangular bipyramid (Figure 6), is not yet known in metal cluster chemistry. The second and third members of the HCP centered at the midpoint of an "octahedral" triangle are known: the face-sharing bioctahedral $[Rh_9(CO)_{19}]^{3-}$[20] (Figure 7) and the bidiminished $\nu_2$ triangular-bipyramidal $[Ni_{12}(CO)_{21}H_{4-n}]^{n-}$[21] (Figure 8).

For the HCP with respect to the center of an octahedral hole, we note the hexacapped octahedral cluster $[Fe_6Pd_6(CO)_{24}H]^{3-}$[22] depicted in Figure 9.

For the BCC there are two types of edges. Both series have been treated here (cf. Table XXV and XXVI). The first and second members of the BCC with respect to the center of a flattened-tetrahedral hole (cf. Table XXVII) are portrayed in parts a and b of Figure 10. The flattened-tetrahedral structure has been observed in $Co_4(NO)_4(NCMe_3)_4$.[23]

Several of the initial clusters in the FCC centered at a lattice point are polyhedral clusters of the type studied in ref 3. Thus the 13-point cluster is a $\nu_1$ cuboctahedron (Figure 4a), the 19-point cluster is a $\nu_2$ octahedron (Figure 11), the 55-point cluster is a $\nu_2$ cuboctahedron, and the 201-point cluster is a $\nu_2$ truncated

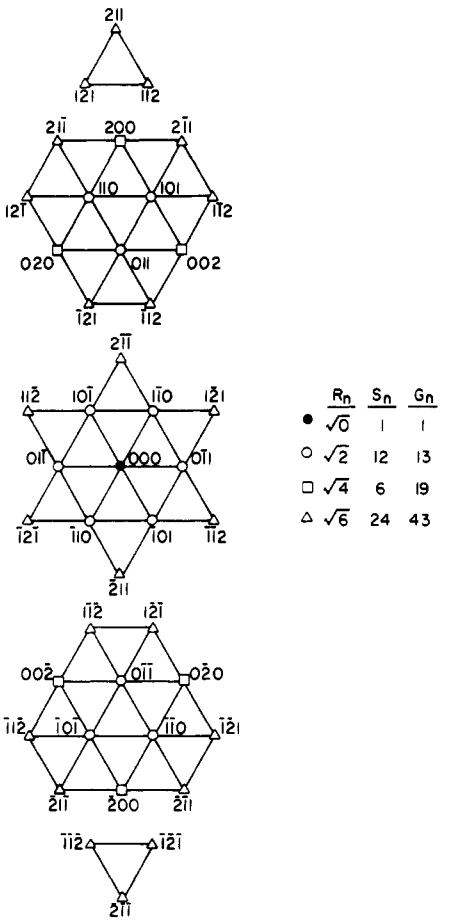


**Figure 13.** FCC centered at a lattice point: a 43-atom cluster.

(20) Martinengo, S.; Fumagalli, A.; Bonfichi, R.; Ciani, G.; Sironi, A. *J. Chem. Soc., Chem. Commun.* **1982**, 825.
(21) Broach, R. W.; Dahl, L. F.; Longoni, G.; Chini, P.; Schultz, A. J.; Williams, J. M. *Transition Metal Hydrides*; Advances in Chemistry 167; American Chemical Society: Washington, DC, 1978; p 93.
(22) Longoni, g.; Manassero, M.; Sansoni, M. *J. Am. Chem. Soc.* **1980**, *102*, 3242.
(23) Gall, R. S.; Connelly, N. G.; Dahl, L. F. *J. Am. Chem. Soc.* **1974**, *96*, 4017.

**Table XVI.**

| $n$ | coords.* | type | $S_n$ | $G_n$ |
|---|---|---|---|---|
| 0 | 000.0 | $L$ | 1 | 1 |
| 2 | $\bar{3}30.0$[6], $2\bar{1}\bar{1}.a$[6] | $L,L'$ | 12 | 13 |
| 4 | $\bar{4}22.a$ | $L'$ | 6 | 19 |
| $5^{1}/_{3}$ | 000,2$a$ | $L$ | 2 | 21 |
| 6 | $\bar{6}33.0$[6], $54\bar{1}.a$[12] | $L,L'$ | 18 | 39 |
| $7^{1}/_{3}$ | $\bar{3}30.2a$ | $L$ | 12 | 51 |
| 8 | $\bar{6}60.0$ | $L$ | 6 | 57 |
| 10 | $\bar{7}52.a$ | $L'$ | 12 | 69 |
| $11^{1}/_{3}$ | $\bar{6}33.2a$ | $L$ | 12 | 81 |
| 12 | $\bar{8}\bar{4}\bar{4}.a$ | $L'$ | 6 | 87 |
| $12^{2}/_{3}$ | $2\bar{1}\bar{1}.3a$ | $L'$ | 6 | 93 |
| $13^{1}/_{3}$ | $\bar{6}60.2a$ | $L$ | 12 | 105 |

**Table XVII.**

| $n$ | coords.* |
|---|---|
| $^{1}/_{2}$ | $\bar{3}30.0$ |
| $1^{1}/_{2}$ | $33\bar{6}.0$[2], $11\bar{2}.a$[2] |
| $2^{1}/_{2}$ | $\bar{5}14.a$ |
| $3^{1}/_{2}$ | $\bar{9}12.0$[4], $7\bar{5}\bar{2}.a$[4] |
| $4^{1}/_{2}$ | $\bar{9}90.0$[2], $7\bar{1}\bar{8}.a$[4] |
| $5^{1}/_{2}$ | $\bar{5}\bar{5}10.a$ |
| $5^{5}/_{6}$ | $\bar{3}30.2a$ |
| $6^{1}/_{2}$ | $93\bar{1}2.0$[4], $\bar{1}\bar{1}74.a$[4] |
| $6^{5}/_{6}$ | $33\bar{6}.2a$ |
| $7^{1}/_{2}$ | $\bar{1}\bar{1}110.a$ |
| $8^{1}/_{2}$ | $\bar{5}13\bar{8}.a$ |
| $8^{5}/_{6}$ | $\bar{9}36.2a$ |

**Table XVIII.**

| $n$ | coords.* |
|---|---|
| $^{1}/_{2}$ | $11\bar{2}.\bar{e}$ |
| $1^{1}/_{2}$ | $5\underline{1}\underline{4}.e$ |
| $2^{1}/_{2}$ | $7\underline{5}\bar{2}.\bar{e}$ |
| $3^{1}/_{6}$ | $11\underline{2}.3e$ |
| $3^{1}/_{2}$ | $7\underline{1}\bar{8}.\bar{e}$ |
| $4^{1}/_{6}$ | $5\underline{1}\underline{4}.3e$ |
| $4^{1}/_{2}$ | $5\underline{5}\bar{1}0.e$ |
| $5^{1}/_{6}$ | $7\underline{5}\bar{2}.3e$ |
| $5^{1}/_{2}$ | $11\underline{7}\bar{4}.e$ |
| $6^{1}/_{6}$ | $7\underline{1}\bar{8}.3e$ |
| $6^{1}/_{2}$ | $11\underline{1}\bar{1}0.e$ |
| $7^{1}/_{6}$ | $55\bar{1}0.3e$ |

**Table XIX.**

| $n$ | coords.* |
|---|---|
| $^{2}/_{3}$ | $\bar{2}11.0$ |
| $1^{1}/_{3}$ | 000.$a$ |
| $2^{2}/_{3}$ | $4\bar{2}\bar{2}.0$ |
| $3^{1}/_{3}$ | $\bar{3}30.a$ |
| $4^{2}/_{3}$ | $\bar{5}41.0$ |
| 6 | $\bar{2}11.2a$ |
| $7^{1}/_{3}$ | $\bar{6}33.a$ |
| 8 | $4\bar{2}\bar{2}.2a$ |
| $8^{2}/_{3}$ | $7\bar{5}\bar{2}.0$ |
| $9^{1}/_{3}$ | $\bar{6}60.a$ |
| 10 | $\bar{5}41.2a$ |
| $10^{2}/_{3}$ | $\bar{8}44.0$ |

**Table XX.**

| $n$ | coords.* |
|---|---|
| $^{2}/_{3}$ | $2\bar{1}\bar{1}.0$ |
| 2 | $2\bar{1}\bar{1}.a$ |
| $2^{2}/_{3}$ | $\bar{4}22.0$ |
| 4 | $4\bar{2}\bar{2}.a$ |
| $4^{2}/_{3}$ | $5\bar{4}\bar{1}.0$ |
| 6 | $2\bar{1}\bar{1}.2a$[6], $4\bar{2}\bar{2}.a$[6] |
| 8 | $\bar{4}22.2a$ |
| $8^{2}/_{3}$ | $\bar{7}52.0$ |
| 10 | $5\bar{4}\bar{1}.2a$[12], $7\bar{5}\bar{2}.a$[12] |
| $10^{2}/_{3}$ | $\bar{8}\bar{4}\bar{4}.0$ |
| 12 | $\bar{8}44.a$ |
| $12^{2}/_{3}$ | $\bar{7}\bar{8}\bar{1}.0$[6], $\bar{2}11.3a$[6] |

**Table XXI.**

| $n$ | coords.* |
|---|---|
| $^{2}/_{3}$ | $\bar{1}\bar{1}2.2\bar{u}$[1], $5\bar{4}\bar{1}.u$[2] |
| $1^{1}/_{3}$ | $\bar{4}\bar{4}8.u$ |
| 2 | $8\bar{1}\bar{7}.2\bar{u}$[2], $55\bar{1}0.u$[1] |
| $2^{4}/_{9}$ | $1\bar{1}2.4u$ |
| $2^{2}/_{3}$ | $\bar{1}0\bar{8}2.\bar{2}u$ |
| $3^{1}/_{3}$ | $\bar{1}0\bar{1}11.\bar{2}u$[2], $\bar{1}358.u$[2] |
| $3^{7}/_{9}$ | $8\bar{1}\bar{7}.4u$ |
| 4 | $14\bar{4}\bar{1}0.u$ |
| $4^{2}/_{9}$ | $5\bar{4}\bar{1}.5u$ |
| $4^{4}/_{9}$ | $\bar{1}0\bar{8}2.4u$ |
| $4^{2}/_{3}$ | $14\bar{1}\bar{3}\bar{1}.u$ |
| $4^{4}/_{9}$ | $\bar{4}\bar{4}8.5u$ |

**Table XXII.**

| $n$ | coords.* |
|---|---|
| $^{1}/_{4}$ | $\bar{2}11.\bar{c}$[3], 000.3$c$[1] |
| $2^{1}/_{12}$ | 000.$5\bar{c}$ |
| $2^{3}/_{4}$ | $4\bar{2}\bar{2}.\bar{c}$[3], $\bar{3}30.3c$[6] |
| $4^{1}/_{12}$ | $\bar{3}30.5\bar{c}$ |
| $4^{3}/_{4}$ | $\bar{5}41.\bar{c}$[6], $\bar{2}11.7c$[3] |
| $6^{3}/_{4}$ | $4\bar{2}\bar{2}.7c$[3], $6\bar{3}\bar{3}.3c$[6] |
| $7^{5}/_{12}$ | $\bar{2}11.9\bar{c}$ |
| $8^{1}/_{12}$ | $6\bar{3}\bar{3}.5\bar{c}$ |
| $8^{3}/_{4}$ | $7\bar{5}\bar{2}.\bar{c}$[6], $\bar{5}41.7c$[6], $\bar{6}60.3c$[6] |
| $9^{5}/_{12}$ | $4\bar{2}\bar{2}.9\bar{c}$ |
| $10^{1}/_{12}$ | $\bar{6}60.5c$[6], 000.11$c$[1] |
| $10^{3}/_{4}$ | $\bar{8}44.\bar{c}$ |

**Table XXIII.**

| $n$ | coords.* |
|---|---|
| 1 | $\bar{2}11.e$ |
| 3 | $\bar{4}22.\bar{e}$ |
| $3^{4}/_{3}$ | $\bar{2}11.3e$ |
| 5 | $\bar{5}41.e$ |
| $5^{2}/_{3}$ | $\bar{4}22.3e$ |
| $7^{4}/_{3}$ | $\bar{5}41.\bar{3}e$ |
| 9 | $\bar{7}52.\bar{e}$[12], $\bar{2}11.5e$[6] |
| 11 | $\bar{8}44.e$[6], $\bar{4}22.\bar{5}e$[6] |
| $11^{2}/_{3}$ | $\bar{7}52.3e$ |
| 13 | $\bar{8}71.e$[12], $\bar{5}41.5e$[12] |
| $13^{3}/_{3}$ | $\bar{8}44.\bar{3}e$ |
| $15^{2}/_{3}$ | $\bar{8}71.\bar{3}e$ |

Table XVI. HCP with respect to point of packing. *First 3 coords. have been multiplied by 3. $a = 2/\sqrt{3}$.

Table XVII. HCP with respect to mid-point of edge within layer. *First 3 coords. have been multiplied by 6. $a = 2/\sqrt{3}$.

Table XVIII. HCP with respect to mid-point of edge between layers. *First 3 coords. have been multiplied by 6. $e = 1/\sqrt{3}$.

Table XIX. HCP with respect to center of triangle between tetrahedra. *First 3 coords. have been multiplied by 3. $a = 2/\sqrt{3}$.

Table XX. HCP with respect to center of triangle between octahedra. *First 3 coords. have been multiplied by 3. $a = 2/\sqrt{3}$.

Table XXI. HCP with respect to center of triangle between layers. *First 3 coords. have been multiplied by 9. $u = 2/(3\sqrt{3})$.

Table XXII. HCP with respect to center of tetrahedral hole. *First 3 coords. have been multiplied by 3. $c = 1/(2\sqrt{3})$.

Table XXIII. HCP with respect to center of octahedral hole. *First 3 coords. have been multiplied by 3. $e = 1/\sqrt{3}$.

**Table XXIV.**

| $n$ | coords. | $S_n$ | $G_n$ |
|---|---|---|---|
| 0 | 000 | 1 | 1 |
| 3 | 111 | 8 | 9 |
| 4 | 200 | 6 | 15 |
| 8 | 220 | 12 | 27 |
| 11 | 311 | 24 | 51 |
| 12 | 222 | 8 | 59 |
| 16 | 400 | 6 | 65 |
| 19 | 331 | 24 | 89 |
| 20 | 420 | 24 | 113 |
| 24 | 422 | 24 | 137 |
| 27 | 333[8], 511[24] | 32 | 169 |
| 32 | 440 | 12 | 181 |

**Table XXV.**

| $n$ | coords.* |
|---|---|
| $^{3}/_{4}$ | 111 |
| $2^{3}/_{4}$ | $\bar{3}11$ |
| $4^{3}/_{4}$ | $\bar{3}\bar{3}1$ |
| $6^{3}/_{4}$ | 511[6], 333[2] |
| $8^{3}/_{4}$ | $5\bar{3}1$ |
| $10^{3}/_{4}$ | $5\bar{3}\bar{3}$ |
| $12^{3}/_{4}$ | $\bar{7}11$[6], 551[6] |
| $14^{3}/_{4}$ | $\bar{7}\bar{3}1$[12], $55\bar{3}$[6] |
| $16^{3}/_{4}$ | 733 |
| $18^{3}/_{4}$ | $\bar{7}51$[12], 555[2] |
| $20^{3}/_{4}$ | 911[6], $\bar{7}\bar{5}3$[12] |
| $22^{3}/_{4}$ | $9\bar{3}1$ |

**Table XXVI.**

| $n$ | coords. |
|---|---|
| 1 | 001 |
| 2 | 110 |
| 5 | 201 |
| 6 | 112 |
| 9 | 221[8], 003[2] |
| 10 | 310 |
| 13 | 203 |
| 14 | 312 |
| 17 | 401[8], 223[8] |
| 18 | 330[4], 114[8] |
| 21 | 421 |
| 22 | 332 |

**Table XXVII.**

| $n$ | coords.* |
|---|---|
| $1^{1}/_{4}$ | 201 |
| $3^{1}/_{4}$ | 203 |
| $5^{1}/_{4}$ | 421 |
| $7^{1}/_{4}$ | 423[8], 205[4] |
| $9^{1}/_{4}$ | 601 |
| $11^{1}/_{4}$ | 603[4], 425[8] |
| $13^{1}/_{4}$ | 641[8], 207[4] |
| $15^{1}/_{4}$ | 643[8], 605[4] |
| $17^{1}/_{4}$ | 821[8], 427[8] |
| $19^{1}/_{4}$ | 823[8], 645[8] |
| $21^{1}/_{4}$ | 607[4], 209[4] |
| $23^{1}/_{4}$ | 825 |

Table XXIV. BCC with respect to lattice point.

Table XXV. BCC with respect to mid-point of edge. *Coords. have been multiplied by 2.

Table XXVI. BCC with respect to mid-point of long edge.

Table XXVII. BCC with respect to center of tetrahedral hole. *Coords. have been multiplied by 2.

octahedron (Figure 12). The 43-point cluster is shown in Figure 13 but is not one of the polyhedra studied in ref 3.

**Electron Counting of High-Nuclearity Close-Packed Clusters.** The atom-counting results presented in this paper greatly facilitate electron counting of metal cluster systems, especially for large clusters where the disposition of atoms within the cluster becomes increasingly difficult to visualize as the cluster size increases.

In Table XXVIII we compare the predicted and the observed electron counts for some representative clusters. In the context of the topological electron counting (TEC)[24-28] rule, a cluster with $V$ vertices ($V = V_n + V_m$, where $V_n$ is the number of main-group atoms and $V_m$ is the number of transition-metal atoms) and $F$ faces

(24) Teo, B. K. *Inorg. Chem.* **1984**, *23*, 1251.
(25) Teo, B. K.; Longoni, G.; Chung, F. R. K. *Inorg. Chem.* **1984**, *23*, 1257.
(26) Teo, B. K. *Inorg. Chem.* **1985**, *24*, 1627.
(27) Teo, B. K. *Inorg. Chem.* **1985**, *24*, 4209.
(28) Teo, B. K., submitted for publication.

**Table XXVIII. Predicted Atom ($G_n$) and Electron ($T$,$B$) Counts for Some Representative Metal Clusters.**

| *Table* | *Fig.* | *n* | $G_n$ | $T$ | $B$ | *Examples* |
|---|---|---|---|---|---|---|
| I | 1(d) | 2 | 9 | | | |
| III | 1(c) | 1/2 | 4 | 32[a] | 8[a] | $Co_4(PPh)_2(CO)_{10}$ [7] |
| V | 1(e) | 1 1/2 | 4 | 31[a] | 7[a] | $[Re_4(CO)_{16}]^{2-}$ [6] |
| VI | 1(a) | 2/3 | 3 | 24[a] | 6[a] | $Os_3(CO)_{12}$ [4] |
| VI | 1(b) | 2 2/3 | 6 | 45[a] | 9[a] | $Os_6(CO)_{17}(P(OMe)_3)_4$ [5] |
| | | | | 42[b] | 6[b] | $Cu_3Fe_3(CO)_{12}^{3-}$ [8] |
| X | 2(e) | 3/4 | 8 | 60[a] | 12[a] | $Ni_8(PPh)_6(CO)_8$ [9] |
| XII,XVIII | 5(a) | 1 1/2 | 6 | 43[a] (42[c]) | 7[a] (6[c]) | $(Ph_3P)_2Au_2Os_4H_2(CO)_{12}$ [17] |
| XII,XVIII | 5(b) | 2 1/2 | 10 | 69[a] | 9[a] | $[Ru_{10}C_2(CO)_{24}]^{2-}$ [18] |
| XIII | 2(a) | 1 1/3 | 4 | 30[a] | 6[a] | $Ir_4(CO)_{12}$ [10] |
| XIII | 2(d) | 2 | 7 | 49[a] | 7[a] | $[Rh_7(CO)_{16}]^{3-}$ [12] |
| XV | 2(c) | 1 | 6 | 43[a] | 7[a] | $Rh_6(CO)_{16}$ [13] |
| XV | | 3 | 14 | 51[a] | 7[a] | $Ti_6O_8Cp_6$ [14] |
| XV | 3 | 5 | 38 | 235[b] | 7[b] | $[Pt_{38}(CO)_{44}H_x]^{2-}$ [15] |
| XVI | 4(b) | 2 | 13 | 85[a,b] | 13[a,b] | $[Rh_{13}(CO)_{24}H_{5-n}]^{n-}$ [16] |
| XVII | 5(c) | 1 1/2 | 6 | | | |
| XVII | 5(d) | 2 1/2 | 10 | | | |
| XIX | 2(b) | 1 1/3 | 5 | 36[a] | 6[a] | $Os_5(CO)_{16}$ [19] |
| XIX | 6 | 2 2/3 | 8 | | | |
| XX | 7 | 2 | 9 | 62[a] (61[c]) | 8[a] (7[c]) | $[Rh_9(CO)_{19}]^{3-}$ [20] |
| XX | 8 | 2 2/3 | 12 | 83[a] | 11[a] | $[Ni_{12}(CO)_{21}H_{4-n}]^{n-}$ [21] |
| XXIII | 9 | 3 | 12 | 79[a] (80[c]) | 7[a] (8[c]) | $[Fe_6Pd_6(CO)_{24}H]^{3-}$ [22] |
| XXVII | 10(a) | 1 1/4 | 4 | 32[a] | 8[a] | $Co_4(NO)_4(NCMe_3)_4$ [23] |
| XXVII | 10(b) | 3 1/4 | 8 | | | |

[a] $T = 3V_n + 8V_m - F + \epsilon + X$; $B = 2V - F + \epsilon + X$ where $\epsilon = 1$ and 2 for 2- and 3-D clusters. See text for the meaning of the symbols. [b] $T_n = 6G_n + K$; $B_n = I_n + K = T_n - 6S_n$. [c] Observed electron counts (shown only if different from the predicted values).

is required to have $T = 3V_n + 8V_m - F + \epsilon + X$ *topological electron pairs*: $\epsilon$ is the Euler characteristic ($\epsilon = 1$ and 2 for 2D and 3D systems, respectively), and $X$ is the "adjustment parameter", which can be determined easily by a set of simple rules.[24] The corresponding number of *skeletal electron pairs* is[26] $B = 2V - F + \epsilon + X$. These equations apply to clusters of low or moderate nuclearity. The predicted values are tabulated in Table XXVIII (with superscript *a*) and compared with the observed values (listed with superscript *c* only if they disagree with the predicted value).

For *close-packed high-nuclearity* metal clusters, the number of topological electron pairs is given by[1,3,26-30] $T_n = 6G_n + K$, where $G_n$ is the total number of metal atoms and $K$ is the $B$ value at the "center" of the cluster. Thus $K = 7, 6, 8, 6, 7, \ldots$ for clusters centered at an atom, a triangle, a square, a tetrahedron, an octahedron, ..., and so on. The corresponding number of shell electron pairs is given by[1,3] either $B_n = 6I_n + K$ or $B_n = T_n - 6S_n$, where $I_n$ ($=G_n - S_n$) and $S_n$ are the numbers of "interior" and "surface" atoms, respectively. The predicted $T_n$ and $B_n$ values (with superscript *b*) for some high-nuclearity metal clusters are also listed in Table XXVIII. For example, the $\nu_2$ triangular cluster $Cu_3Fe_3(CO)_{12}^{3-}$ [8] is centered on a triangle; hence, $T_n = 6 \times 6 + 6 = 42$, which agrees with the observed value of $(3 \times 11 + 3 \times 8 + 12 \times 2 + 3)/2 = 42$ electron pairs. Note that this value is three electron pairs short of the 45 predicted by the TEC rule (the latter was observed in $Os_6(CO)_{17}(P(OMe)_3)_4$ [5]). The truncated-octahedral cluster $[Pt_{38}(CO)_{44}H_x]^{2-}$ [15] is predicted to have $T_n = 6 \times 38 + 7 = 235$ electron pairs since it is centered at an octahedral hole, in good agreement with the observed value of $(38 \times 10 + 44 \times 2 + x + 2)/2 = 235 + x/2$. Finally, the twinned-cuboctahedral cluster $[Rh_{13}(CO)_{24}H_{5-n}]^{n-}$ is predicted to have $T_n = 6 \times 13 + 7 = 85$ electron pairs, which agrees with the observed value of $(13 \times 9 + 24 \times 2 + 5)/2 = 85$.

**Predictions of Electron Counts for Clusters and Crystallites.** It is tempting to predict the atom and electron counts for *high-nuclearity close-packed* metal clusters of a given arrangement. This is done in Table XXIX for the following representative packing arrangements: (I) the hexagonal lattice with respect to the center of a triangle (cf. Table VI); (II) the FCC with respect to an atom (cf. Table XI); (III) the FCC with respect to an octahedral hole (cf. Table XV); (IV) the HCP with respect to an atom (cf. Table XVI). The total atom counts ($G_n$) are taken from Tables I–XXVII (see also ref 1), and the $T_n$ values (the total electron pair counts) are calculated[1,3] from $T_n = 6G_n + K$ (vide supra).

**Table XXIX. Predicted Total Atom ($G_n$) and Total Electron Pair ($T_n$) Counts of High Nuclearity Close-Packed Clusters for Some Representative Packings: (I) Hexagonal with respect to a Triangle (Table 6)[a]; (II) FCC with respect to an Atom (Table 11)[b]; (III) FCC with respect to an Octahedral Hole (Table 15)[c]; (IV) HCP with respect to an Atom (Table 16)[d].**

| I | | II | | III | | IV | |
|---|---|---|---|---|---|---|---|
| $G_n$ | $T_n$ | $G_n$ | $T_n$ | $G_n$ | $T_n$ | $G_n$ | $T_n$ |
| 3 | 24 | 1 | - | 6 | 43 | 1 | - |
| 6 | 42 | 13 | 85 | 14 | 91 | 13 | 85 |
| 12 | 78 | 19 | 121 | 38 | 235 | 19 | 121 |
| 18 | 114 | 43 | 265 | 68 | 415 | 21 | 133 |
| 21 | 132 | 55 | 337 | 92 | 559 | 39 | 241 |
| 27 | 168 | 79 | 481 | 116 | 703 | 51 | 313 |
| 30 | 186 | 87 | 529 | 164 | 991 | 57 | 349 |
| 36 | 222 | 135 | 817 | 188 | 1135 | 69 | 421 |
| 42 | 258 | 141 | 853 | 236 | 1423 | 81 | 493 |
| 48 | 294 | 177 | 1069 | 266 | 1603 | 87 | 529 |
| 54 | 330 | 201 | 1213 | 298 | 1795 | 93 | 565 |
| 63 | 384 | 225 | 1357 | 370 | 2227 | 105 | 637 |

[a] $T_n = 6G_n + 6$. [b,c,d] $T_n = 6G_n + 7$.

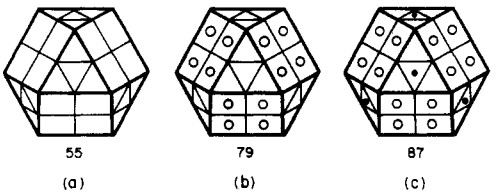


**Figure 14.** FCC centered on an atom: (a) 55-atom cluster; (b) 79-atom cluster; (c) 87-atom cluster.

The size and shape of some of the clusters listed in Table XXIX have already been discussed. Interestingly, none of the clusters obtained from the FCC centered on an atom (Table XI) are known in metal cluster chemistry. The predicted electron-pair counts are listed in Table XXIX. For example, the 43-, 55-, and 201-atom clusters are predicted to require a total ($T_n$) of 265, 337, and 1213 electron pairs or 530, 674, and 2426 electrons, respectively. It would be a challenge to synthesize these high-nuclearity clusters even with the knowledge of the electronic requirements. The lower members of the series (or any series) will no doubt be synthesized in due course. A more funadmental, and perhaps more important, question is to determine at which point there is not enough room for the ligands to satisfy the required electron count. Consider the example platinum carbonyl clusters. The predicted $Pt_{43}$, $Pt_{55}$, and $Pt_{201}$ will require $(530 - 43 \times 10)/2 = 50$, $(674 - 55 \times 10)/2 = 62$, and $(2426 - 201 \times 10)/2 = 208$ carbonyls or equivalent ligands or negative charges, respectively. These clusters have respectively 37, 42, and 122 surface atoms. While it is conceivable that one might be able to fit $\lesssim 50$ carbonyls on the 37 surface atoms of the $Pt_{43}$ cluster (similarly with $Pt_{55}$), it is difficult to see how one could fit $\lesssim 208$ carbonyls on the 122 surface atoms of the $Pt_{201}$ cluster. Perhaps for such high nuclearities, the clusters may (1) adopt more open structures will more corners and edges instead of spherically shaped structures, (2) make use of interstitial ligands such as hydrides, carbides, nitrides, etc., (3) convert to bulk-like electronic requirements so that they are no longer governed by cluster rules, etc. Perhaps at some point the distinction between large metal clusters and small metal

(29) Strictly speaking, $T_n$, $B_n$, and $S_n$ correspond to $T$, $B$, and $V_m$ in ref 26 (cf. eq 7) *only* for small clusters, where $B$ can be considered as the number of either the *bonding cluster orbitals* or, in terms of electrons filling these orbitals, the *skeletal electron pairs* (cf. ref 6 of ref 26 in this paper). For larger clusters, this connection is lost and $B_n$ is better described as the number of *shell electron pairs*.

(30) Ciani, G.; Sironi, A. *J. Organomet. Chem.* **1980**, *197*, 233.

Table XXX. Some Possible Arrangements for the Magic Numbers Observed in Xenon Clusters.[a]

| Magic Number | Spherical Clusters[b] | Polyhedral Clusters[c] |
|---|---|---|
| 13 | FCC on atom<br>HCP on atom | $\nu_1$ cuboctahedron<br>$\nu_1$ twinned cuboctahedron<br>$\nu_1$ icosahedron |
| 19 | cubic on atom<br>FCC on atom<br>FCC on triangle<br>HCP on atom or triangle | $\nu_2$ octahedron |
| 25 | FCC on triangle<br>HCP on triangle between layers | |
| 55 | FCC on atom | $\nu_2$ cuboctahedron<br>$\nu_2$ icosahedron<br>$\nu_4$ square pyramid |
| 81 | cubic on atom<br>HCP on atom<br>HCP on triangle between octahedra or layers | |
| 87 | FCC on atom<br>HCP on atom<br>HCP on triangle between octahedra | |
| 135 | FCC on atom<br>HCP on atom<br>HCP on triangle between octahedra | |
| 147 | cubic on atom<br>HCP on atom | $\nu_3$ icosahedron |

[a] Ref. 31g. [b] This work and ref. 1. [c] ref. 3. [d] Non-closed-shell. [e] See ref. 32-34.

particles will vanish as covalent metal–ligand bonds and chemisorbed ligands on the surface of a cluster/crystallite become indistinguishable.

**Cluster Beams.** In a cluster-beam experiment[31] the clusters are formed by nucleation in a supersaturated vapor phase via adiabatic expansion into a vacuum. The clusters are often analyzed by time-of-flight mass spectrometry. It has been observed that, for a certain value of the nuclearity (often referred to by the experimentalists as magic numbers), the intensity exhibits a local maximum, indicating enhanced stability or ease of formation for a closed-shell structure. The results of the present paper can sometimes aid in interpreting such experimental data. For example, the magic numbers observed for the sphere packing of xenon atoms in a cluster-beam experiment[31g] are 13, 19, 25, 55, 71, 81, 87, 135, 147, etc. (cf. Table XXX). As pointed out by the authors of that paper, "if the clusters grow in the FCC structure, one might expect magic numbers for clusters having complete shells, i.e., $n$ = 13, 19, 43, 55, 79, 87, 135, 141, 177, ...". The latter series corresponds to the FCC lattice centered on an atom (see Table XI). The absence of certain numbers in the series (viz., $n$ = 43, 79, 141) was taken as evidence contradicting the assumption that clusters in this size range already possess bulk (FCC) structure. On the other hand, all the magic numbers predicted for icosahedral clusters (13, 19, 55, and 147) were observed, and the authors asserted that these clusters were formed by icosahedral growth. While we agree with these authors in their interpretation, we would like to offer suggestions regarding the possible atomic arrangements of all the prominent magic numbers, including those that are less readily explained by the icosahedral growth mechanism. This is summarized in Table XXX, where the various possible closed-shell arrangements are listed for each magic number observed.

The prominent magic number 71 is rather interesting in that it does not fit into any of the series considered here or elsewhere. It is tempting to suggest that it is a truncated polyhedron derivable from that corresponding to the 79-atom cluster (Figure 14b) in the FCC centered on an atom since it is halfway between 55 (Figure 4a) and 87 (Figure 14c). One such *possible* arrangement for a 71-atom cluster is depicted in Figure 15, where 8 atoms have been removed from two square faces of the 79-atom cluster. Other non-closed-shell truncated polyhedra (cf. this work and ref 3) can also be considered. For example, the 25-atom cluster, in addition to the closed-shell arrangements indicated in Table XXX, can also be considered as a truncated 43-atom cluster (Figure 13) by removing the top two layers and the bottom layer (43 − 3 − 12 − 3 = 25).

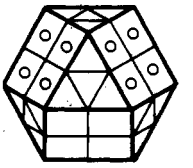

71

**Figure 15.** Possible atomic arrangement for a 71-atom cluster with FCC close packing via removal of eight atoms from the 79-atom cluster shown in Figure 14b.

Finally, the 19- and 25-atom clusters, again in addition to the possible arrangements suggested in Table XXX, may also be considered as arising from one-dimensional fused (interpenetrating) icosahedral or pentagonal growth as observed in cluster chemistry (e.g. $Au_{13}$,[32] $Pt_{19}$,[33] and $Au_{13}Ag_{12}$[34] clusters).

It seems that the magic numbers observd in cluster-beam experiments often cannot be completely explained by a single growth mechanism, even for inert-gas clusters, where sphere packing and van der Waals interactions are probably the dominant factors in dictating the shape of the clusters. We take this as manifestation that more often than not there is more than one operative cluster growth mechanism.

**Catalysis and Surface Science.** The atom-counting results presented in this paper may be applied to the determination of (1) the number of atoms and the geometry of a given site and (2) the coordination numbers (or local environment). This information is extremely important in *catalysis* and *surface science*, since it is generally believed that the former controls whether or not a certain *reaction* or *adsorption* can take place on the site, whereas the latter relates to the *activity* or the *rate* of the process. In this context, our work was preceded by the pioneering work of van Hardeveld and Hartog[35] and others.[36] These authors provided extensive statistical data concerning the *number* and *types* of surface atoms and their environment as a function of crystallite size for crystals with FCC, BCC, and HCP structures. They also gave certain formulas for the numbers of surface and bulk atoms and the total number of atoms as the nuclearity increases (in a way similar to but less general than our previous work[3,37]). On the basis of these results, these authors considered the influence of crystallite size on the sorptive and catalytic behavior of metal catalysts.

While our work differs from that of van Hardeveld and Hartog in many respects, it can be applied in a similar way to catalysis and surface science.

(31) (a) Ozin, G. A.; Mitchell, S. A. *Angew. Chem., Int. Ed. Engl.* **1983**, *22*, 674. (b) Dietz, T. G.; Duncan, M. A.; Powers, D. E.; Smalley, R. E. *J. Chem. Phys.* **1981**, *74*, 6511. (c) Rohlfing, E. A.; Cox, D. M.; Kaldor, A. *Chem. Phys. Lett.* **1983**, *99*, 161. (d) Knight, W. D. *Surf. Sci.* **1981**, *106*, 172. (e) Martin, T. P. *Phys. Rep.* **1983**, *95*, 167. (f) Kappes, M. M.; Kunz, R. W.; Schumacher, E. *Chem. Phys. Lett.* **1982**, *91*, 413. (g) Echt, O.; Sattler, K.; Recknagel, E. *Phys. Rev. Lett.* **1981**, *47*, 1121.

(32) Briant, C. E.; Theobald, B. R. C.; White, J. W.; Bell, L. K.; Mingos, D. M. P.; Welch, A. J. *J. Chem. Soc., Chem. Commun.* **1981**, *201*.

(33) Washecheck, D. M.; Wucherer, E. J.; Dahl, L. F.; Ceriotti, A.; Longoni, G.; Manassero, M.; Sansoni, M.; Chini, P. *J. Am. Chem. Soc.* **1979**, *101*, 6110.

(34) Teo, B. K.; Keating, K. *J. Am. Chem. Soc.* **1984**, *106*, 2224.

(35) van Hardeveld, R.; Hartog, F. *Surf. Sci.* **1969**, *15*, 189.

(36) Poltorak, O. M.; Boronin, V. S. *Russ. J. Phys. Chem.* (*Engl. Transl.*) **1966**, *40*, 1436.

(37) Note that the definition of nuclearity ($m$) of van Hardeveld and Hartog[35] differs from ours ($n$) by unity; viz., $m = n + 1$.

**Other Applications.** The results concerning the numbers and types of atoms and their coordinates may also be useful in understanding the morphology and habits of microcrystallites[38] and the structure (cavities) and properties of zeolites and clays[39] and in investigating the electronic structure[40] of metal clusters and the dynamic simulation[41] of crystal and cluster growth, as well as in many branches of science involving sphere packing.

The results presented in this paper should also be useful in spectroscopic techniques such as extended X-ray absorption fine structure (EXAFS)[42] and low-energy electron diffraction (LEED),[43] where, in addition to the numbers and types of atoms, the site geometry, symmetry, and coordination numbers are important parameters to be applied to, or deduced from, experimental data.

**Acknowledgment.** We thank Dr. J. Sinfelt of Exxon Research and Engineering Co., Annandale, NJ, for bringing van Hardeveld and Hartog's pioneering work to our attention.

(38) See, for example: *Crystal Form and Structure*; Schneer, C. J., Ed.; Dowden, Hutchinson and Ross: Stroudsburg, PA, 1977.
(39) See, for example: (a) Breck, D. W. *Zeolite Molecular Sieves*; Wiley: New York, 1974. (b) *Zeolite Chemistry and Catalysis*; Rabo, J. A., Ed.; ACS Monograph 171, American Chemical Society: Washington, DC, 1976. (c) Barrer, R. M. *Zeolites and Clay Minerals as Sorbents and Molecular Sieves*; Academic: London, 1978. (d) *Molecular Sieves*; Meier, W. M., Uytterhoeven, J. B., Eds.; Advances in Chemistry 121; American Chemical Society: Washington, DC, 1973. (e) *Molecular Sieves-II*; Katzer, J. R., Ed.; ACS Symposium Series 40; American Chemical Society: Washington, DC, 1977. (f) *Intrazeolite Chemistry*; Stucky, G. D., Dwyer, F. G., Eds.; ACS Symposium Series 218; American Chemical Society: Washington, DC, 1983.
(40) See, for example: (a) Hoffmann, R. *Angew. Chem., Int. Ed. Engl.* **1982**, *21*, 71. (b) Lauher, J. W. *J. Am. Chem. Soc.* **1978**, *100*, 5305; **1979**, *101*, 2604. (c) Ciani, G.; Sironi, A. *J. Organomet. Chem.* **1980**, *197*, 233. (d) Mingos, D. M. P. *J. Chem. Soc., Dalton Trans.* **1974**, *133*; **1976**, 1163. (e) Teo, B. K.; Hall, M. B.; Fenske, R. F.; Dahl, L. F. *J. Organomet. Chem.* **1974**, *70*, 413; *Inorg. Chem.* **1975**, *14*, 3103. (f) Yang, Y. C.; Johnson, K. H.; Salahub, D. R.; Kaspar, J.; Messmer, R. P. *Phys. Rev. B: Condens. Matter* **1981**, *24*, 5673 and references cited therein.
(41) See, for example: (a) Hoare, M. R. *Adv. Chem. Phys.* **1979**, *40*, 49. (b) Hoare, M. R.; McInnes, J. A. *Adv. Phys.* **1983**, *32*, 791. (c) Hoare, M. R.; Pal, P. *Nature (London), Phys. Sci.* **1972**, *236*, 35. (d) Hoare, M. R.; Pal, P. *J. Cryst. Growth* **1972**, *17*, 71.
(42) See for example: Teo, B. K. *EXAFS: Basic Principles and Data Analysis*; Springer-Verlag: Heidelberg, West Germany, 1986. *EXAFS Spectroscopy: Techniques and Applications*; Teo, B. K., Joy, D. C., Eds.; Plenum: New York, 1981. *EXAFS and Near Edge Structure*; Bianconi, A., Incoccia, L., Stipcich, S., Eds.; Springer-Verlag: Heidelberg, West Germany, 1983; and references cited therein.
(43) See, for examples: (a) Pendry, J. B. *Low Energy Electron Diffraction*; Academic: New York, 1974. (b) Van Hove, M. A.; Tong, S. Y. *Surface Crystallography by LEED*; Springer-Verlag: West Berlin, 1979.

Contribution from the Istituto di Ricerca sulle Onde Elettromagnetiche del CNR, 50127 Firenze, Italy

# Systems Exhibiting Spin Equilibrium. Do Different Chromophores Really Coexist in the Lattice?

M. Bacci

*Received June 5, 1985*

Depending upon the strength of the coupling between two different pure spin states, a double or a single minimum can occur on the potential energy surface of the ground state. In the former case two different chromophores can be revealed by suitable fast experiments, while in the latter the whole system behaves as if constituted by chromophores of only one kind in the presence of large anharmonicity. As an example the problem of the singlet-triplet spin equilibrium in iron(II) complexes is considered.

## Introduction

The strength of the ligand field (LF) governs the ground-state spin multiplicity in transition-metal complexes having electronic configurations $d^2$, $d^3$, ..., $d^8$. When the LF splitting is comparable with the interelectronic repulsion, high-spin (HS) and low-spin (LS) states are nearly degenerate and an anomalous magnetic behavior has to be expected, with magnetic moments intermediate between those of purely HS and LS complexes.

Since the first examples reported by Cambi and his school in the early 1930s,[1] many compounds with "anomalous" magnetic moment have been described, particularly in the chemistry of iron(II), iron(III), and cobalt(II).[2-5] In spite of the vast amount of experimental data that is now available, a full description of these systems has not yet been reached and several issues are still open. One of these issues concerns the effective coexistence of HS and LS species or, in other words, the possibility of distinguishing the simultaneous presence of HS and LS complexes in the lattice by using suitable experiments.[4-19] When intermolecular mechanisms induce phase transitions, it is obvious that two alternative species can be identified in the two phases. The situation is quite different when no apparent phase transition occurs. With regard to X-ray diffraction studies two extremes have been described: (i) a multiple-temperature analysis has revealed the coexistence of two spin isomers for the methanol solvate of tris(2-picolylamine)iron(II) dichloride;[19] on the contrary, (ii) the crystal structures of the $[Fe(P_4)Br]BPh_4 \cdot CH_2Cl_2$ complex ($P_4$ = hexaphenyl-1,4,7,10-tetraphosphadecane) at 298 and 150 K have shown only one species with "normal" thermal ellipsoids in the lattice.[6,11] Moreover, spectroscopic measurements can provide a double or a single signal, and in the latter case, usually it is said that the lifetimes of the coexisting spin isomers are shorter than

(1) Cambi, L.; Cagnasso, A. *Atti Accad. Naz. Lincei, Cl. Sci. Fis., Mat. Nat., Rend.* **1931**, *13*, 809. Cambi, L.; Szegö, L. *Ber. Dtsch. Chem. Ges.* **1931**, *64*, 259; **1933**, *66*, 656. Cambi, L.; Szegö, L.; Cagnasso, A. *Atti Accad. Naz. Lincei, Cl. Sci. Fis., Mat. Nat.*, Rend. **1932**, *15*, 266, 329.
(2) König, E. *Coord. Chem. Rev.* **1968**, *4*, 471.
(3) Martin, R. L.; White, A. H. *Transition Met. Chem. (N.Y.)* **1968**, *4*, 113.
(4) Goodwin, H. A. *Coord. Chem. Rev.* **1976**, *18*, 293.
(5) Gütlich, P. *Struct. Bonding (Berlin)* **1981**, *44*, 83.
(6) Bacci, M.; Ghilardi, C. A.; Orlandini, A. *Inorg. Chem.* **1984**, *23*, 2798.
(7) Golding, R. M.; Whitfield, H. J. *Trans. Faraday Soc.* **1966**, *62*, 1713.
(8) Merrithew, P. B.; Rasmussen, P. G. *Inorg. Chem.* **1972**, *11*, 325.
(9) Cox, M.; Darken, J.; Fitzsimmons, B. W.; Smith, A. W.; Larkworthy, L. F.; Rogers, K. A. *J. Chem. Soc., Dalton Trans.* **1972**, 1192.
(10) Leipoldt, J. G.; Coppens, P. *Inorg. Chem.* **1973**, *12*, 2269.
(11) Bacci, M.; Ghilardi, C. A. *Inorg. Chem.* **1974**, *13*, 2398.
(12) König, E.; Ritter, G.; Goodwin, H. A. *Chem. Phys. Lett.* **1975**, *31*, 543.
(13) Hall, G. R.; Hendrickson, D. N. *Inorg. Chem.* **1976**, *15*, 607.
(14) Gatteschi, D.; Ghilardi, C. A.; Orlandini, A.; Sacconi, L. *Inorg. Chem.* **1978**, *17*, 3023.
(15) Cecconi, F.; Di Vaira, M.; Midollini, S.; Orlandini, A.; Sacconi, L. *Inorg. Chem.* **1981**, *20*, 3423.
(16) Kremer, S.; Henke, W.; Reinen, D. *Inorg. Chem.* **1982**, *21*, 3013.
(17) König, E.; Ritter, G.; Kulshreshtha, S. K.; Nelson, S. M. *Inorg. Chem.* **1982**, *21*, 3022.
(18) König, E.; Ritter, G.; Kulshreshtha, S. K.; Waigel, J.; Sacconi, L. *Inorg. Chem.* **1984**, *23*, 1241.
(19) Katz, B. A.; Strouse, C. E. *J. Am. Chem. Soc.* **1979**, *101*, 6214.

0020-1669/86/1325-2322$01.50/0 